NANO LETTERS

Letter

pubs.acs.org/NanoLett

Rational Synthesis of Ultrathin n-Type Bi_2Te_3 Nanowires with Enhanced Thermoelectric Properties

Genqiang Zhang,[†] Benjamin Kirk,[‡] Luis A. Jauregui,[§,∥] Haoran Yang,[†] Xianfan Xu,[‡] Yong P. Chen,[§,∥,⊥] and Yue Wu*[,†]

[†]School of Chemical Engineering, [‡]School of Mechanical Engineering, [§]School of Electrical and Computer Engineering, [∥]Birck Nanotechnology Center, [⊥]Department of Physics, Purdue University, West Lafayette, Indiana, United States

Supporting Information

ABSTRACT: A rational yet scalable solution phase method has been established, for the first time, to obtain n-type Bi_2Te_3 ultrathin nanowires with an average diameter of 8 nm in high yield (up to 93%). Thermoelectric properties of bulk pellets fabricated by compressing the nanowire powder through spark plasma sintering have been investigated. Compared to the current commercial n-type Bi_2Te_3-based bulk materials, our nanowire devices exhibit an enhanced ZT of 0.96 peaked at 380 K due to a significant reduction of thermal conductivity derived from phonon scattering at the nanoscale interfaces in the bulk pellets, which corresponds to a 13% enhancement compared to that of the best n-type commercial $Bi_2Te_{2.7}Se_{0.3}$ single crystals (~0.85) and is comparable to the best reported result of n-type $Bi_2Te_{2.7}Se_{0.3}$ sample (ZT = 1.04) fabricated by the hot pressing of ball-milled powder. The uniformity and high yield of the nanowires provide a promising route to make significant contributions to the manufacture of nanotechnology-based thermoelectric power generation and solid-state cooling devices with superior performance in a reliable and a reproducible way.

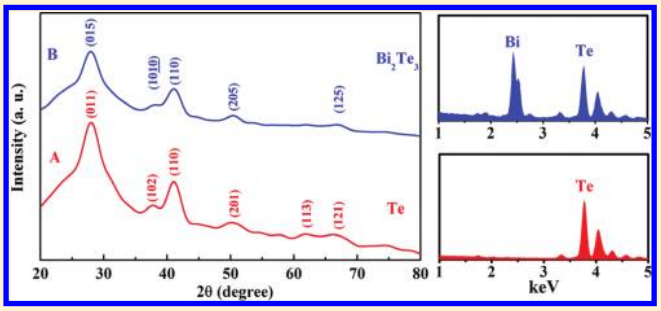

KEYWORDS: *Bi_2Te_3, nanowires, thermoelectric, spark plasma sintering*

Thermoelectric materials, which can generate electricity by recovering waste heat or be used as solid-state cooling devices, have attracted a lot of attention recently due to their great potential to improve energy efficiency for military and civilian applications.[1] The main challenge in this area is to create high-performance materials as defined by the thermoelectric figure of merit, $ZT = S^2\sigma T/\kappa$, where S is the thermoelectric power or Seebeck coefficient of the material, σ and κ are electrical conductivity and thermal conductivity, respectively, and T is the average temperature between the hot and the cold ends. There has been tremendous progress towards enhancing thermoelectric properties through different ways, including exploiting new types of high-performance complicated bulk crystals, such as skutterudite[2] and $CsBi_4Te_6$,[3] or applying nanostructure engineering, such as superlattice films,[4] embedded nanograins in bulk $AgPb_mSbTe_{2+m}$ materials,[5] and so on. Among various techniques, one-dimensional nanowires have been considered one of the most promising routes to obtain better ZT values through the sharp enhancement of electron density of states due to quantum confinement and the significant reduction of thermal conductivity due to increased surface/interface scattering of phonons.[6−8] Notably, theoretical studies indicate that there is a strong relationship between thermoelectric properties and nanowire diameter, and the ZT value could even be enhanced to higher than 6 if nanowires with diameters around 5 nm could be achieved. At the same time, in order for nanowire-based thermoelectric materials to have a real technology impact, a rational yet scalable synthetic approach has to be developed. Indeed, many effective routes to fabricate various ultrathin nanowires have been investigated, ranging from noble metals[9,10] and sulfides[11−13] to oxides,[14,15] but most of them have extremely low yield and typically require complicated growth procedures.

We focus our research on bismuth telluride (Bi_2Te_3) because Bi_2Te_3 and its related alloys, including p-type $Bi_xSb_{2-x}Te_3$ and n-type $Bi_2Te_{3-x}Se_x$, still remain as the best thermoelectric materials close to room temperature[16,17] and because the maximum ZT of n-type bulk $Bi_2Te_{3-x}Se_x$ is around 0.85.[16] Recently, Ren et al. successfully increased the ZT of n-type $Bi_2Te_{2.7}Se_{0.3}$ to 1.04 by increasing the electrical conductivity through the reorientation of ab planes of small crystals in a multiple-step hot pressing of ball-milled nanopowder.[18] Here, we report a different approach to improve the ZT of n-type Bi_2Te_3 through a two step synthesis of ultrathin n-type Bi_2Te_3 nanowires with an average diameter around 8 nm. The simplicity, scalability, and extremely high yield of the nanowires with uniform diameter have enabled us to use spark plasma sintering (SPS) to consolidate nanowire powder into bulk

Received: August 23, 2011
Revised: October 21, 2011
Published: November 23, 2011

   dx.doi.org/10.1021/nl202935k | *Nano Lett.* 2012, 12, 56−60

pellets to test their thermoelectric performance, and an optimized ZT value of 0.96 peaked at 380 K has been achieved.

The ultrathin Bi_2Te_3 nanowires are synthesized by a two-step solution phase reaction in which we grow ultrathin Te nanowires first and then perform a diffusion reaction to diffuse Bi into the Te nanowire templates to form the compound nanowires. For the synthesis of Te nanowires, 20 mL of ethylene glycol is added to a three-neck flask equipped with a standard Schlenk line, followed by adding of 0.2 g of polyvinylpyrrolidone (PVP, M_w ~40 000), 0.6 g of NaOH, and 3 mmol of TeO_2 powder (99.999%). The mixture is heated to 160 °C with nitrogen protection, and then 0.6 mL of hydrazine hydrate is added to the above solution as a reducing agent. Uniform Te nanowires are formed in 1 h. A Bi precursor solution is made by dissolving 2 mmol of $Bi(NO_3)_3 \cdot 5H_2O$ into 5 mL of ethylene glycol. For the synthesis of Bi_2Te_3 nanowires, the as-prepared Bi precursor solution is injected into the above Te nanowire solution at 160 °C. After another 1 h reaction, Bi_2Te_3 nanowires are obtained. The overall yield of the Bi_2Te_3 nanowires calculated from the starting precursors is estimated to be as high as 93%, which truly demonstrates the potential for scaling-up of this simple yet straightforward synthetic approach.

After the synthesis, we characterized the as-obtained Te nanowires and Bi_2Te_3 nanowires using various methods. Figure 1 shows the typical X-ray diffraction (XRD) patterns of the Te nanowires and the Bi_2Te_3 nanowires, which can be readily indexed to pure Te phase (JCPDS no. 36-1452) and pure Bi_2Te_3 phase (JCPDS no. 65-3750). The peaks for both of these two materials are quite broad mainly due to the finite size of our products. Notably, the similarity of crystal structures between Te and Bi_2Te_3 also makes it difficult to identify the difference between Te and Bi_2Te_3 directly from the XRD patterns. Therefore, energy dispersive X-ray spectroscopy (EDS) analysis is performed on both of these materials, the results of which are shown on the right of the corresponding XRD patterns. Indeed, a significant amount of Bi is observed in the nanowires after Bi precursor injection, giving an atomic ratio between Bi:Te of around 36:64 in our final product, which means the Bi_2Te_3 nanowire we got through the two-step procedure is Te-rich Bi_2Te_3 phase. The chemical composition has also been confirmed by the X-ray photoelectron spectroscopy (XPS) measurements (Figure S1, Supporting Information). The atomic ratio of Bi and Te calculated from XPS results is around 35.7:64.3, which is consistent with that of EDS results. A slight surface oxidation has also been observed on Bi_2Te_3 nanowire sample in XPS study,[19,20] which happens due to the unavoidable exposure to oxygen during the sample transfer after removing the capping ligands.

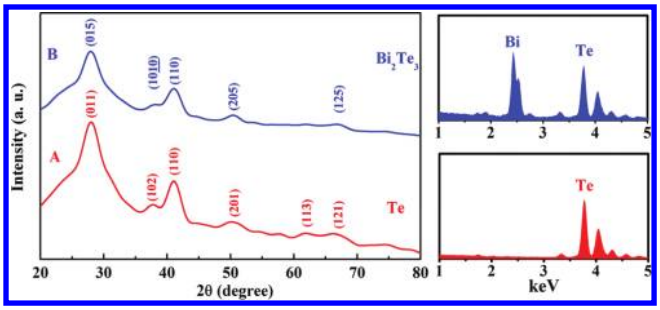

Figure 1. Typical XRD patterns and corresponding EDS spectrum of (A) Te and (B) Te-rich Bi_2Te_3 nanowires.

Transmission electron microscopy (TEM) has also been used to characterize the morphology, size, and crystallinity of our intermediate and final products. Low-resolution TEM studies shown in Figure 2A,B performed on the intermediate products obtained after the first step of the reaction show the formation of uniform Te nanowires with an average diameter of 5 nm. The uniformity of the Te nanowires is demonstrated by size distribution analysis, as shown in Figure 2C, giving a narrow diameter distribution of 5 ± 1 nm. High-resolution TEM (HRTEM) studies (inset, Figure 2B) confirm that the observed nanowires are Te with a growth direction of ⟨001⟩, which results from its highly anisotropic crystal structure along the *c*-axis.[21−23] Typical TEM images and size distribution for the products obtained after the injection of Bi precursor

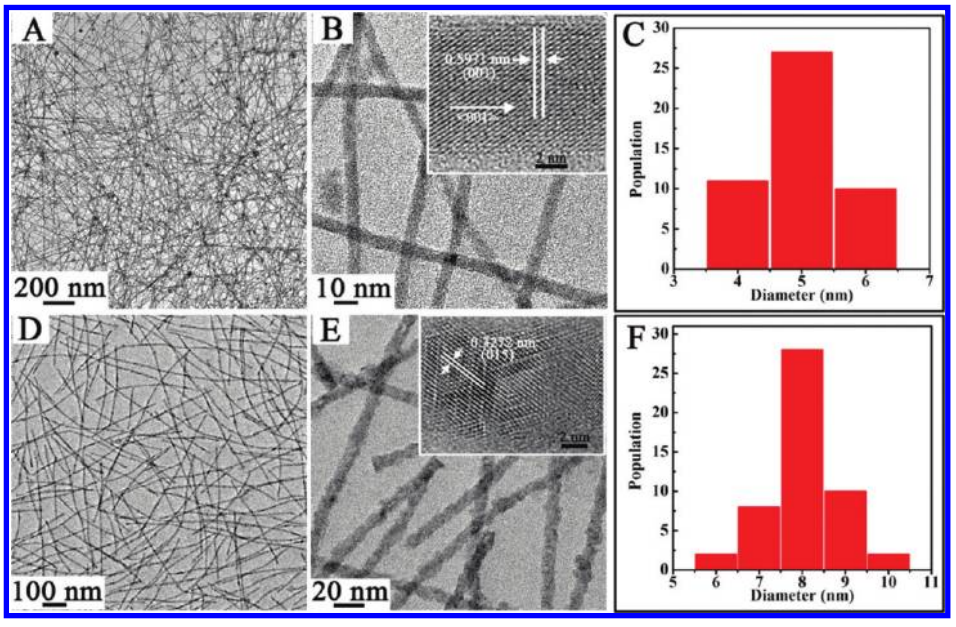

Figure 2. TEM images and size distribution analyses for (A−C) Te and (D−F) Te-rich Bi_2Te_3 nanowires. The insets in (B) and (E) are HRTEM images for Te and Bi_2Te_3 nanowires, respectively.

dx.doi.org/10.1021/nl202935k | *Nano Lett.* 2012, 12, 56−60

solution are shown in Figure 2D−F, which demonstrate that both the morphology and the uniformity of the nanowires are retained after converting the Te phase to the Bi_2Te_3 compound. However, there are three important features for Bi_2Te_3 nanowires based on analysis of the TEM results: First, the average diameter of the nanowires increases from 5 to 8 nm, although the size distribution is still narrow, as shown in Figure 2F. Notably, our Bi_2Te_3 nanowires have a much thinner diameter compared to previous report on the Bi_2Te_3 nanowires synthesized through the reaction between triphenylbismuthine and Te nanowires, which is simply because of the much smaller diameter of our Te nanowires.[24] Second, unlike the Te nanowires with smooth surfaces (Figure 2A,B), the Bi_2Te_3 nanowires exhibit quite rough surfaces. Third, different from single crystalline nature of Te nanowires, the final Bi_2Te_3 nanowires clearly exhibit multiple crystalline domains with many dislocations, as shown in the inset of Figure 2E. The labeled lattice fringes in Figure 2E could be indexed to the (015) crystal planes for Bi_2Te_3 phase. A possible reason for the polycrystalline nature of Bi_2Te_3 nanowires is the unit cell volume change due to the large lattice expansion in *c*-axis after converting Te to the Bi_2Te_3 phase. During this process, the unit cell volume will increase around 5 times and generate large strain, which will result in the formation of polycrystalline domains and lattice dislocation so that the strain inside the nanowires can be released and could also partially contribute to the peak broadening in XRD analysis.

The high yield of the uniform Bi_2Te_3 nanowires gives us the opportunity to investigate their potential thermoelectric application by using SPS to compress the dry Bi_2Te_3 nanowire powder into bulk pellets. In a typical fabrication process, we first remove the capping ligands on Bi_2Te_3 nanowires by combining the nanowires dispersed in ethanol with diluted hydrazine solution (10% volume ratio) and stirring vigorously until all the nanowires are precipitated. The supernatant is decanted, and the precipitate is washed with ethanol three times to remove hydrazine. After the hydrazine treatment, the nanowires are collected by centrifugation, dried in vacuum, and consolidated by SPS at 678 K for 5 min under an axial pressure of 50 MPa and a dc current of 15 kA into bulk pellets with 2.54 cm in diameter and around 0.25 cm in thickness with a relative density of ∼80%.

Figure 3 shows the typical electrical and thermal properties of the nanowire bulk pellets after SPS. The detailed description of the measurements is included in the Supporting Information. The electrical conductivity (Figure 3A) decreases from 50.75×10^3 S/m at 300 K to 42.31×10^3 S/m at 400 K. The electrical conductivity of our nanowire composites is lower than that of recently reported n-type $Bi_2Te_{2.7}Se_{0.3}$ samples fabricated by hot pressing of ball-milled powder,[18] which is mainly due to the smaller diameter/grain size in our ultrathin nanowires. The negative sign of the Seebeck coefficient shown in Figure 3B indicates that our Te-rich Bi_2Te_3 ultrathin nanowires are n-type thermoelectric materials, which is consistent with previous literatures.[25,26] The absolute value of the Seebeck coefficient gradually increases from 205 μV/K at 300 K to 245 μV/K at 400 K, which is slightly higher than that of the hot-pressed n-type $Bi_2Te_{2.7}Se_{0.3}$ sample.[18] A power factor ($S^2\sigma$, Figure 3C) of 21.4×10^{-4} $Wm^{1-}K^{-2}$ at room temperature is achieved, and it gradually increases to 25.2×10^{-4} $Wm^{1-}K^{-2}$ at 390 K mainly due to the enhancement of Seebeck coefficient along with increasing temperature. Figure 3D shows the temperature dependence of thermal conductivity in the temperature range

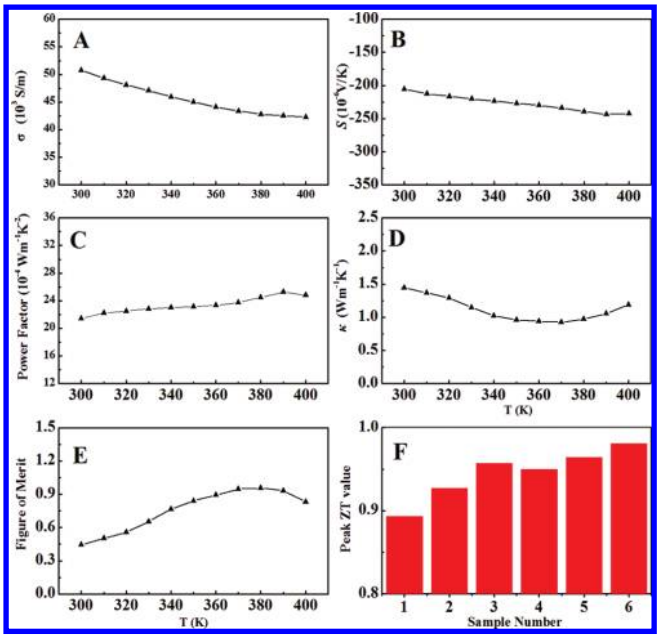

Figure 3. Thermoelectric property measurement of Bi_2Te_3 nanowire composites after SPS treatment: temperature dependence of (A) electrical conductivity; (B) Seebeck coefficient; (C) power factor; (D) thermal conductivity; (E) ZT calculation; and (F) typical peak ZT value distributions observed from multiple Bi_2Te_3 nanowire bulk pellets.

from 300 to 400 K. The thermal conductivity is 1.42 $Wm^{1-}K^{-1}$ at 300 K and decreases to 0.92 $Wm^{1-}K^{-1}$ at 370 K. After that, the thermal conductivity starts to increase and reaches 1.19 $Wm^{1-}K^{-1}$ at 400 K. The value of thermal conductivity observed in our nanowire bulk pellets is much lower than that of the best n-type commercial $Bi_2Te_{2.7}Se_{0.3}$ single crystals (∼1.65 $Wm^{1-}K^{-1}$).[27] The increase of thermal conductivity after 370 K is related with the bipolar effect in Bi−Te alloy system,[28] which has also been well documented in other reports.[18,29] Based on the above measurements, we calculate the ZT of our Te-rich Bi_2Te_3 nanowire composites, which is shown in Figure 3E. The peak ZT value is around 0.96 at 380 K, corresponding to a 13% enhancement compared to that of the best n-type commercial $Bi_2Te_{2.7}Se_{0.3}$ single crystals (∼0.85) and comparable to the best reported result of n-type $Bi_2Te_{2.7}Se_{0.3}$ sample (ZT = 1.04) fabricated by hot pressing of ball-milled powder.[18] Most importantly, to the best of our knowledge, this ZT value is significantly higher than the previously reported values from solution processed thermoelectric materials,[30−32] and our approach does not require any time-consuming energy-intensive manufacture and external doping. More significantly, the statistic distribution of ZT values (Figure 3F) measured from multiple nanowire bulk pellets is quite narrow (within 10%), which further proves the uniformity of our nanowires and provides a reliable and reproducible manufacture route for high-performance thermoelectric devices.

We attribute the high performance of our nanowire thermoelectric devices to the SPS, which is a pressure-assisted rapid sintering process using a pulsed dc to produce spark discharges to heat samples under high pressure and to press the nanowires into monoliths. Instead of taking the risk of forming larger crystal grains in the long-time conventional thermal annealing, the SPS approach is a much faster process that has several advantages: (1) It will prevent the growth of grain size

dx.doi.org/10.1021/nl202935k | *Nano Lett.* 2012, 12, 56−60

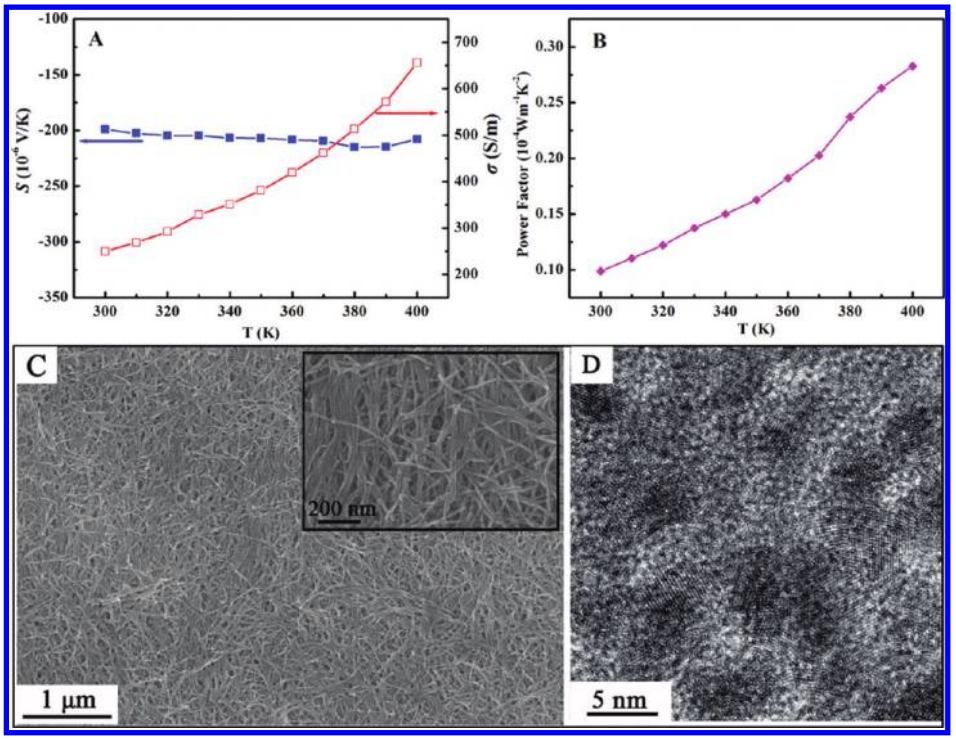

Figure 4. (A) Temperature dependence of Seebeck coefficient and electrical conductivity. (B) Calculated power factor for n-type Bi_2Te_3 nanowire drop-casted films. (C) Typical scanning electron microscopy images for Bi_2Te_3 nanowire film, the inset is an enlarged view of the morphology. (D) Typical HRTEM images for Bi_2Te_3 nanowire composites after SPS process.

while still creating extensive connections between the compacted nanowires to reduce the electrical resistivity; (2) it will lower thermal conductivity through phonon scattering at nanoscale boundaries (nanowire interfaces); and (3) it will help to achieve better mechanical strength and improved isotropy. These advantages have been observed when we compare the SPS samples to the thin film samples made by drop casting the nanowire solution onto glass substrates. Figure 4A shows the temperature dependence of electrical conductivity and Seebeck coefficient results obtained from the drop-casted nanowire thin film annealed at 678 K, indicating a much lower electrical conductivity of (~249 S/m at 300K and 655 S/m at 400 K) , while a similar Seebeck coefficient compared with those of SPS treated nanowire bulk pellets, from the calculated power factor of Bi_2Te_3 drop-casted thin film (Figure 4B), is nearly two orders lower. Structural characterization performed on the drop-casted nanowire thin film (Figure 4C) shows that indeed the film made by drop-casting consists of randomly bundled Bi_2Te_3 nanowires with increased diameter in a loosely layered stack structure even after a conventional thermal annealing at 678 K. The SPS-fabricated nanowire bulk pellets (Figure 4D), however, have the randomly oriented and interlaced nanowire feature retained with nanoscale grains (~8 nm) even after the nanowires are fully compressed into bulk pellets, which shows nearly no overgrowth from the original diameter of our Bi_2Te_3 nanowires, and the existence of nanoscale grain boundaries will strongly favor the phonon scattering to reduce the thermal conductivity.

In conclusion, we have developed a facile solution phase method to successfully obtain ultrathin Te-rich Bi_2Te_3 nanowires with a yield as high as 93%. The synthetic approach requires neither special reactor vessels nor high-pressure/high-temperature conditions and thus is suitable for scaling up in the industrial standard batch reactors for mass production. The thermoelectric property measurement results indicate that the thermal conductivity for SPS-processed nanowire sample is much lower than that of the bulk materials due to the enhanced phonon scattering at the nanoscale interfaces, which results in a 13% enhancement of the ZT value compared to that of the best commercial n-type $Bi_2Te_{2.7}Se_{0.3}$ bulk crystals. This simple solution phase reaction to produce uniform ultrathin nanowires in high yield, together with an optimized spark plasma sintering process to consolidate the nanowire powder into bulk pellets, could become a promising route to make significant contribution to the manufacture of nanotechnology-based thermoelectric power generation and solid-state cooling devices with superior performance in a reliable and a reproducible way.

■ ASSOCIATED CONTENT

Ⓢ Supporting Information

XPS measurements. Electrical and thermal properties of the nanowire bulk pellets after SPS. This material is available free of charge via the Internet at http://pubs.acs.org.

■ AUTHOR INFORMATION

Corresponding Author

*E-mail: yuewu@purdue.edu. Telephone: 765-494-6028.

■ ACKNOWLEDGMENTS

Y.W. thanks the support from the Purdue University new faculty startup grant, the Midwest Institute of Nanoelectronic Discovery (MIND), and the DuPont Young Faculty Award. Y.W. and X.X. acknowledge the support from the NSF/DOE Thermoelectric Partnership (award number 1048616). Y.P.C. thanks the support from the MIND, the Purdue Cooling Technologies Research Center, and Intel Corporation. Y.W. thanks Dr. Douglas Dudis and Charles Cooke at Wright-

Patterson Air Force Research Lab for the help on the spark plasma sintering of nanowire powder.

REFERENCES

(1) Bell, L. E. *Science* **2008**, *321*, 1457.
(2) Uher, C. Skutterudite: ProspectiVe Novel Thermoelectrics in Recent Trends in Thermoelectric Materials Research I. *Semiconductors and Semimetals*; Tritt, T. M, Ed.; Academic Press: San Diego, CA, 2001, *69*, 139.
(3) Chung, D. Y.; Hogan, T.; Brazis, P.; Rocci-Lane, M.; Kannewurf, C.; Bastea, M.; Uher, C.; Kanatzidis, M. G. *Science* **2000**, *287*, 1024.
(4) Venkatasubramanian, R.; Siivola, E.; Colpitts, T.; O'Quinn, B. *Nature* **2001**, *413*, 597.
(5) Hsu, K. F.; Loo, S.; Guo, F.; Chen, W.; Dyck, J. S.; Uher, C.; Hogan, T.; Polychroniadis, E. K.; Kanatzidis, M. G. *Science* **2004**, *303*, 818.
(6) Hicks, L. D.; Dresselhaus, M. S. *Phys. Rev. B* **1993**, *47*, 16631.
(7) Hicks, L. D.; Dresselhaus, M. S. *Phys. Rev. B* **1993**, *47*, 12727.
(8) Lin, Y. M.; Dresselhaus, M. S. *Phys. Rev. B* **2003**, 68.
(9) Hong, B. H.; Bae, S. C.; Lee, C. W.; Jeong, S.; Kim, K. S. *Science* **2001**, *294*, 348.
(10) Huo, Z. Y.; Tsung, C. K.; Huang, W. Y.; Zhang, X. F.; Yang, P. D. *Nano Lett.* **2008**, *8*, 2041.
(11) Cademartiri, L.; Ozin, G. A. *Adv. Mater.* **2009**, *21*, 1013.
(12) Cademartiri, L.; Malakooti, R.; O'Brien, P. G.; Migliori, A.; Petrov, S.; Kherani, N. P.; Ozin, G. A. *Angew. Chem., Int. Ed.* **2008**, *47*, 3814.
(13) Zhang, Y. J.; Xu, H. R.; Wang, Q. B. *Chem. Commun.* **2010**, *46*, 8941.
(14) Yang, Y. F.; Jin, Y. Z.; He, H. P.; Ye, Z. Z. *CrystEngComm* **2010**, *12*, 2663.
(15) Xi, G. C.; Ye, J. H. *Inorg. Chem.* **2010**, *49*, 2302.
(16) Goldsmid, H. J. *Thermoelectric Refrigeration*; Plenum Press: New York, 1964.
(17) Nolas, G. S.; Sharp, J.; Goldsmid, H. J. *Thermoelectrics: Basic Principles and New Materials Developments Springer Series in Material Science 45*; Springer: Berlin, Germany, 2001, 111.
(18) Yan, X. A.; Poudel, B.; Ma, Y.; Liu, W. S.; Joshi, G.; Wang, H.; Lan, Y. C.; Wang, D. Z.; Chen, G.; Ren, Z. F. *Nano Lett.* **2010**, *10*, 3373.
(19) Bando, H.; Koizumi, K.; Oikawa, Y.; Daikohara, K.; Kulbachinskii, V. A.; Ozaki, H. *J. Phys.: Condens. Matter* **2000**, *12*, 5607.
(20) Purkayastha, A.; Kim, S.; Gandhi, D. D.; Ganesan, P. G.; Borca-Tasciuc, T.; Ramanath, G. *Adv. Mater.* **2006**, *18*, 2958.
(21) Zhang, B.; Hou, W. Y.; Ye, X. C.; Fu, S. Q.; Xie, Y. *Adv. Funct. Mate.r* **2007**, *17*, 486.
(22) Tang, Z. Y.; Wang, Y.; Sun, K.; Kotov, N. A. *Adv. Mater.* **2005**, *17*, 358.
(23) Zhang, G. Q.; Yu, Q. X.; Yao, Z.; Li, X. G. *Chem. Commun.* **2009**, 2317.
(24) Yu, H.; Gibbons, P. C.; Buhro, W. E. *J. Mater. Chem.* **2004**, *14*, 595.
(25) Fleurial, J. P.; Gailliard, L.; Triboulet, R.; Scherrer, H.; Scherrer, S. *J. Phys. Chem. Solids* **1988**, *49*, 1237.
(26) Fleurial, J. P.; Gailliard, L.; Triboulet, R.; Scherrer, H.; Scherrer, S. *J. Phys. Chem. Solids* **1988**, *49*, 1249.
(27) Carle, M.; Pierrat, P.; Lahalle-Gravier, C.; Scherrer, S.; Scherrer, H. *J. Phys. Chem. Solids* **1995**, *56*, 201.
(28) Yang, J. In *Thermal conductivity*; Tritt, T. M., Ed.; Springer, New York, 2004, Chap. 1.
(29) Rhyee, J. S.; Cho, E.; Ahn, K.; Lee, K. H.; Lee, S. M. *Appl. Phys. Lett.* **2010**, 97.
(30) Scheele, M.; Oeschler, N.; Meier, K.; Kornowski, A.; Klinke, C.; Weller, H. *Adv. Funct. Mater.* **2009**, *19*, 3476.
(31) Kovalenko, M. V.; Spokoyny, B.; Lee, J. S.; Scheele, M.; Weber, A.; Perera, S.; Landry, D.; Talapin, D. V. *J. Am. Chem. Soc.* **2010**, *132*, 6686.
(32) Wang, R. Y.; Feser, J. P.; Gu, X.; Yu, K. M.; Segalman, R. A.; Majumdar, A.; Milliron, D. J.; Urban, J. J. *Chem. Mater.* **2010**, *22*, 1943.